

Anti-Inflammatory Effects of Clarstatin, a Shared-Epitope–Antagonistic Cyclic Peptide, on Experimental Autoimmune Uveitis in Mice

Shira Merzbach,¹ Adi Schumacher-Klinger,¹ Michal Klazas,¹ Amnon Hoffman,¹ Philip Lazarovici,¹ Chaim Gilon,² Gabriel Nussbaum,³ and Radgonde Amer⁴

¹Institute for Drug Research, School of Pharmacy, Faculty of Medicine, The Hebrew University of Jerusalem, Jerusalem, Israel

²Institute of Chemistry, The Hebrew University of Jerusalem, Jerusalem, Israel

³Institute of Dental Sciences, Hebrew University-Hadassah Faculty of Dental Medicine, Ein Kerem, Jerusalem, Israel

⁴Department of Ophthalmology, Hadassah Medical Center, Faculty of Medicine, Hebrew University of Jerusalem, Jerusalem, Israel

Correspondence: Radgonde Amer, Department of Ophthalmology, Hadassah Medical Center, Faculty of Medicine, Hebrew University of Jerusalem, P.O. Box 12000, Jerusalem 9112001, Israel; radgonde@gmail.com.

Received: August 6, 2024

Accepted: November 26, 2024

Published: January 7, 2025

Citation: Merzbach S, Schumacher-Klinger A, Klazas M, et al. Anti-inflammatory effects of clarstatin, a shared-epitope–antagonistic cyclic peptide, on experimental autoimmune uveitis in mice. *Invest Ophthalmol Vis Sci*. 2025;66(1):13. <https://doi.org/10.1167/iovs.66.1.13>

PURPOSE. Polymorphism and mutations of human leukocyte antigens (HLAs) and calreticulin are risk factors for uveitis. Here, we sought to determine the therapeutic effects of Clarstatin, a cyclic peptide antagonist of the HLA shared-epitope–calreticulin interaction, in experimental autoimmune uveitis (EAU) models.

METHODS. Mice were injected with Clarstatin intraperitoneally and its effect was compared to that of corticosteroid. EAU was evaluated clinically and histologically. Ocular infiltration of CD45⁺ hematopoietic cells and splenocyte CD4⁺ expression were determined using immunofluorescence and flow cytometry (fluorescence-activated cell sorting [FACS]). ELISA was used to measure the ocular level of the proinflammatory cytokines.

RESULTS. Clarstatin significantly ameliorated the severity of EAU in the C57BL/6J mild and the B10.RIII severe mice models. There was a significant dose and time-dependent decrease, in the range of 30% to 80%, in the clinical score ($P < 0.05$), histological score ($P < 0.05$), and number of retinal and spleen CD45⁺ cells ($P < 0.05$ and $P < 0.001$, respectively), a comparable effect to corticosteroid. Clarstatin reduced the intraocular levels of interleukin 6 (IL-6; $P < 0.05$) and monocyte chemoattractant protein-1 (MCP-1; $P < 0.01$) by 41% and 59%, respectively.

CONCLUSIONS. Systemic delivery of Clarstatin significantly improved mild and severe EAU. Its potential anti-inflammatory therapeutic effects represent a novel mode of treatment in ocular inflammation. It may also be a relevant treatment modality in systemic autoimmune conditions in which calreticulin plays a role in their pathogenesis.

Keywords: anti-inflammatory effect, Clarstatin, cyclic peptide drug lead, experimental autoimmune uveitis, shared-epitope–peptidomimetic antagonist

Non-infectious uveitis encompasses a group of potentially blinding, autoimmune inflammatory eye diseases that are induced by infiltrating T lymphocytes capable of recognizing retinal antigens.¹ The incidence and prevalence are highest among patients of working age, posing a significant socioeconomic impact.² Current treatment guidelines³ recommend corticosteroids as the first-line therapy. Additional immunomodulatory (IMT) and biological therapies are needed to control chronic or severe conditions and to avoid corticosteroid-associated adverse effects.⁴ Despite the numerous pharmacotherapeutic options, posterior uveitis remains a significant challenge to treat. There is an unmet clinical need to develop novel IMT therapies that are safe and effective and that act by reducing ocular inflammatory cell infiltration by novel mechanisms of action.⁵

Experimental autoimmune uveitis (EAU) is an eye-specific, T-cell-mediated disease that is characterized by

inflammation and subsequent destruction of the neural retina and adjacent tissues.⁶ Mild and severe EAU can be induced in different strains of rodents by immunization with a retinal antigen such as interphotoreceptor retinoid-binding protein (IRBP).⁷ EAU resembles some human posterior uveoretinitis syndromes such as sympathetic ophthalmia and Vogt–Koyanagi–Harada disease.⁸ Lymphocyte infiltration into the posterior segment of the eye in EAU models is governed by the activation of inflammatory CD45⁺ cells.⁹ Recruitment of these cells to the eye is a fundamental step in EAU development, but no drugs are yet available in the clinic to selectively target and inhibit this process.

Clarstatin is a thiourea-bridged backbone cyclic peptide drug lead recently developed by us. It is comprised of a five-amino-acid sequence¹⁰ based on a motif referred to as “shared epitope” (SE), present in specific alleles of the *HLA-DRB1* gene.¹¹ It has been documented that polymorphic

and mutational SE alleles are linked to uveitis susceptibility.^{12–15} The SE peptide binds to the cell-surface calreticulin (CS-CRT),¹⁶ triggering innate immune signaling.¹⁷ CS-CRT is a multifunctional endoplasmic reticulum calcium-binding protein that is also located on the cell surface of activated T cells, contributing to the development of autoimmune inflammatory diseases.¹⁸ Calreticulin has been implicated in several autoimmune processes via molecular mimicry, epitope spreading, complement inactivation, and stimulation of inflammatory mediators, such as nitric oxide (NO) production.¹⁹ Therefore, inhibitors of human leukocyte antigen (HLA)-SE/CS-CRT interaction such as Clarstatin, represent a new class of drugs for the therapy of autoimmune inflammatory diseases, as previously documented by us in experimental rheumatoid arthritis models.^{20–22} Therefore, in the present study, we sought to investigate the therapeutic effects of Clarstatin on mild and severe EAU mice models clinically and histopathologically and to assess ocular levels of proinflammatory mediators and infiltrating CD45⁺ leukocytes.

MATERIALS AND METHODS

Materials

Human IRBP(161–180) (SGIPYIISYLHPGNTILHVD), and IRBP(1–20) (GPTHLFQPSLVLDMAKVLLD), purity > 98%, were purchased from Adar Biotech Co. (Rehovot, Israel). Pertussis toxin (PTX) was obtained from List Labs (Campbell, CA, USA). A heat-killed *Mycobacterium tuberculosis* strain H37Ra and complete Freund's adjuvant (CFA) were obtained from BDL (Bethesda, MD, USA). DMSO (D2650), protease inhibitor cocktail (P8340), and bovine deoxyribonuclease I (D5025) were purchased from Sigma-Aldrich, (St. Louis MO, USA). Collagenase D (50-100-3282) was obtained from Roche Diagnostics (Mannheim, Germany). Clarstatin was synthesized to 98% purity by solid-phase peptide synthesis applying fluorenylmethoxycarbonyl protecting group (Fmoc) chemistry by Shanghai Yaxian Chemical (Jiading, Shanghai). Methylprednisolone (Solu-Medrol 125 mg/2 mL; Pfizer, New York, NY, USA) and eye drops (cyclopentolate hydrochloride 1%, oxybuprocaine hydrochloride 0.4%, tropicamide 0.5%, and phenylephrine hydrochloride 2.5%) were purchased from the pharmacy of the Hadassah Medical Center (Jerusalem, Israel). Hanks' balanced salt solution (HBSS; 02-016-1A), Dulbecco's modified Eagle's medium (DMEM; 01-055-1A), fetal bovine serum (FBS; 04-001-1A), L-glutamine (03-020-1B), penicillin G sodium and streptomycin sulfate (03-031-1B) were obtained from Biological Industries (Beit-Haemek, Afula, Israel). The monoclonal antibodies anti-mouse CD45 (FITC, 11-0451-82) and anti-mouse CD4 (APC-eFlour 780, 47-0042-82), used for fluorescence-activated cell sorting (FACS) analysis, were sourced from eBioscience (San Diego, CA, USA). The anti-mouse calreticulin monoclonal antibody (ab22683), rabbit anti-mouse CD45 monoclonal antibody (ab208022), secondary polyclonal antibodies goat anti-mouse (Alexa Fluor 488, ab150117) and goat anti-rabbit (Alexa Fluor 594, ab150080), and mounting medium with 4',6-diamidino-2-phenylindole (DAPI; ab104139) used for immunofluorescence were sourced from Abcam (Cambridge, UK). The cytokines and chemokines were measured with the MILLIPLEX MAP Mouse Cytokine/Chemokine (MCYTOMAG-70K) ELISA kit purchased from MilliporeSigma (Billerica, MA, USA).

Animal Models, Experimental Autoimmune Uveitis Induction, and Treatments

Female C57BL/6J mice (6–8 weeks, 16–19 g) were purchased from Envigo (Jerusalem, Israel). Female B10.RIII mice (6–8 weeks, 16–19 g) were purchased from The Jackson Laboratory (Bar Harbor, ME, USA). Animals were maintained with standard chow and water ad libitum in the specific-pathogen free animal research facility of the Faculty of Medicine. EAU experiments were approved by the Hebrew University-Hadassah Institutional Animal Care and Use Committee (MD-20-16345-2) and were conducted in accordance with the ARVO Statement for the Use of Animals in Ophthalmic and Vision Research.

Induction of EAU in C57BL/6J Mild Model and in B10RIII Severe Model

In this study, 122 C57BL/6J and 41 B10RIII female mice were immunized subcutaneously with 500 µg IRBP(1–20) or 50 µg IRBP(161–180), respectively, emulsified with CFA, and 2.5-mg/mL *Mycobacterium tuberculosis* H37Ra. An intraperitoneal (IP) injection of 1 µg of PTX was administered to each mouse.²³ Control mice received phosphate-buffered saline (PBS). Mice were sacrificed at day 35 (C57BL/6J) or day 14 (B10RIII) post-immunization. One eye was collected for histopathological analysis, and the retina of the other eye was used for immunological characterization by FACS.²³ The intraocular levels of the inflammatory mediators were measured by multiplex ELISA.²⁴

Treatments

Experimental groups included mice with disease (EAU-disease, untreated control) and mice with disease and treated with Clarstatin (CL) IP once or three times a week (C57BL/6J mice; 0.0036, 0.036, 0.18, and 0.36 mg/kg body weight; $n = 8, 8, 10$, and 5 , respectively) or three times a week (B10RIII mice; 0.36 or 1 mg/kg body weight; $n = 10$). The effective dose range of Clarstatin was determined based on previous study.¹⁰ The third group included mice with disease which were treated with methylprednisolone (MP) IP (20 mg/kg), three times a week as the positive control. Finally, the fourth group included mice not immunized, (wild-type, healthy, control). The first dose was given 24 hours following EAU induction. The EAU-disease untreated group received IP PBS vehicle solution in the same volume (0.05 mL) as the treated mice.

Clinical Evaluations

Fundus examinations and photography were performed 14 and 28 days following immunization to assess disease progression. Mice were anesthetized by ketamine (85 mg/kg) and xylazine (15 mg/kg) IP. Pupils were dilated with 1% cyclopentolate hydrochloride. EAU clinical scores were evaluated by an ophthalmologist masked to the treatment, using the MICRON-III retina imaging system (Phoenix-Micron, Bend, OR, USA), based on the number, type, size of lesions, and the extent of inflammation. EAU clinical scores were graded from 0 to 4 as described by Thureau et al.²⁵

Hematoxylin and Eosin Staining

At days 14 or 35, the eyeballs were collected, prefixed for 24 hours in Davidson's solution,²⁶ dehydrated in alcohol, and embedded in paraffin. Tissue sections of 3 to 6 μ m were stained with hematoxylin and eosin (H&E). The severity of uveitis was evaluated histologically and graded by a researcher masked to the treatment, using a scale from 0 to 4, as described by Thureau et al.²⁵

Isolation of Retina and Spleen Cells

The eyes were enucleated, and retinas were dissected, washed, cut into small pieces, and digested for 20 minutes at 37°C in 1 mL washing HBSS medium with 2% FBS and with 0.5-mg/mL collagenase D and 750-U/mL DNase I. An additional 10-minute treatment with the same enzymes followed. Next, the cell suspensions were forced through a BD Falcon 40- μ m cell strainer (BD Biosciences, Bedford, MA, USA) using a syringe plunger and then stained with antibodies in the dark for 30 minutes at 2° to 8°C for FACS. To isolate immune cells, the spleens were mechanically mashed and suspended in washing DMEM medium supplemented with 10% FCS, 2 mM L-glutamine, 50,000 units penicillin G sodium, and 50 mg streptomycin sulfate, forced through a 40- μ m cell strainer, and then stained for FACS. The samples were analyzed on a LSRFortessa flow cytometer (BD Biosciences), and the data were analyzed using FCS Express software.^{23,27}

Evaluation of Intraocular Levels of Cytokines

Each dissected eye and intraocular content were scraped into 50- μ L Krebs-Ringer solution with a proteinase inhibitor cocktail diluted 1:100 on ice. They were then mechanically homogenized for 10 strokes and briefly sonicated for 30 pulses of 1 second each. The soluble fraction was collected by centrifugation at 10,000 rpm for 10 minutes at 4°C and then stored at -80°C.²⁴ Interleukin-6 (IL-6) and monocyte chemoattractant protein-1 (MCP-1) levels were measured using the MILLIPLEX MAP mouse cytokine/chemokine assay according to the manufacturer's instructions and normalized to the eye weight.

Immunofluorescence Staining

For deparaffinization, the paraffin sections were heated to 60°C for 15 minutes, then incubated in xylene at room temperature (RT) for 15 minutes. The sections were sequentially transferred into 100%, 95%, 70%, and 50% ethanol for 4 minutes each at RT. Afterward, the sections were rinsed in deionized water and stored in PBS. Antigen retrieval was performed using a buffer containing 10-mM citrate (pH 6.2), 2-mM EDTA, and 0.05% Tween 20. The samples were incubated overnight at 4°C with the goat anti-mouse calreticulin and rabbit anti-mouse CD45 monoclonal antibodies. After washing, the slides were treated for 1 hour at RT with goat anti-mouse (Alexa Fluor 488; green) and goat anti-rabbit (Alexa Fluor 594; red) secondary polyclonal antibodies at 1/1000 dilution. DAPI was used to stain the cell nuclei (blue). Imaging was conducted using a Zeiss LSM 710 Confocal Laser Scanning microscope (Zeiss, Oberkochen, Germany) and Zeiss Axiovert 135M microscope, equipped with a Plan-Apochromat Zeiss 63x lens.²⁸

Statistical Analysis

Data are presented as mean \pm standard error of the mean (SEM) and were considered significant for $P < 0.05$. All experiments were independently repeated at least three times. Statistical analysis was performed using one-way ANOVA followed by Tukey's multiple comparisons, using Prism 5.0 (GraphPad Software, Boston, MA, USA).

RESULTS

Clarstatin Ameliorated Ocular Inflammation and Pathology in the EAU C57BL/6J Mice Model

Mice were immunized with IRBP and PTX, inducing EAU that was clinically assessed 2 and 4 weeks post-immunization; histopathological evaluations were performed at day 35 post-immunization (study endpoint). Figure 1A (top) presents the fundus photographs and Figure 1A (bottom) presents histopathological sections after induction of EAU. The therapeutic effect of Clarstatin or corticosteroid was quantified using the EAU clinical score.⁷ On day 28, an average score of 2.9 was noted for untreated mice compared to a score of 0 for the wild-type mice (Fig. 1B). Mice treated with Clarstatin once a week (2.0; $P = 0.05$) or three times a week (1.9; $P < 0.05$) or corticosteroids three times a week (1.3; $P < 0.001$) showed a significant reduction in the clinical score, indicating an amelioration of the EAU severity by 31%, 36%, and 57%, respectively. Figures 1A (bottom) and 1C depict the anti-inflammatory effects of Clarstatin evaluated histopathologically. In the untreated EAU mice, active uveitis was noted, depicted by the presence of vitreous cells, foci of retinal infiltrates, retinal folding, and vasculitis. Significant amelioration of EAU features was observed in the eyes of Clarstatin- and corticosteroid-treated mice. Figure 1C depicts the corresponding quantitative EAU histological scores of healthy, untreated, and treated mice. Untreated mice had an average score of 1.5 and healthy mice had a score of 0. Markedly reduced scores were noted in EAU-treated mice—Clarstatin once a week (0.8; $P < 0.05$), three times a week (0.7; $P < 0.05$), or corticosteroid (0.5; $P < 0.01$)—with the scores significantly decreasing by 50%, 53%, and 67%, respectively, when compared to the untreated, EAU-disease mice group. The dose-dependent therapeutic effect of Clarstatin evaluated histopathologically is presented in Figure 1D. Clarstatin significantly reduced the structural damage at the doses of 0.036 mg/kg and 0.36 mg/kg, where its effect with the higher dose was comparable to the corticosteroid-positive control. Cumulatively, these results indicated a considerable reduction in the severity of EAU by Clarstatin in the EAU model of C57BL/6J mice.

Clarstatin Inhibited Retinal Infiltration of Leukocytes in EAU-Disease C57BL/6J Mice

In EAU, the hematopoietic T cells coexpressing CD45⁺ (leukocyte common antigen, pan-leukocyte marker) and CD4⁺ (helper T-cell common antigen) represent 63% of the total hematopoietic cell population. These cells infiltrate the eye and drive inflammation and eye damage.²⁹ Therefore, we sought to measure the level of these subset populations in the retina and spleen in mice treated with Clarstatin 5 weeks post-immunization.³⁰ Immunofluorescence was performed on a retinal section of a healthy (unimmunized) mouse,

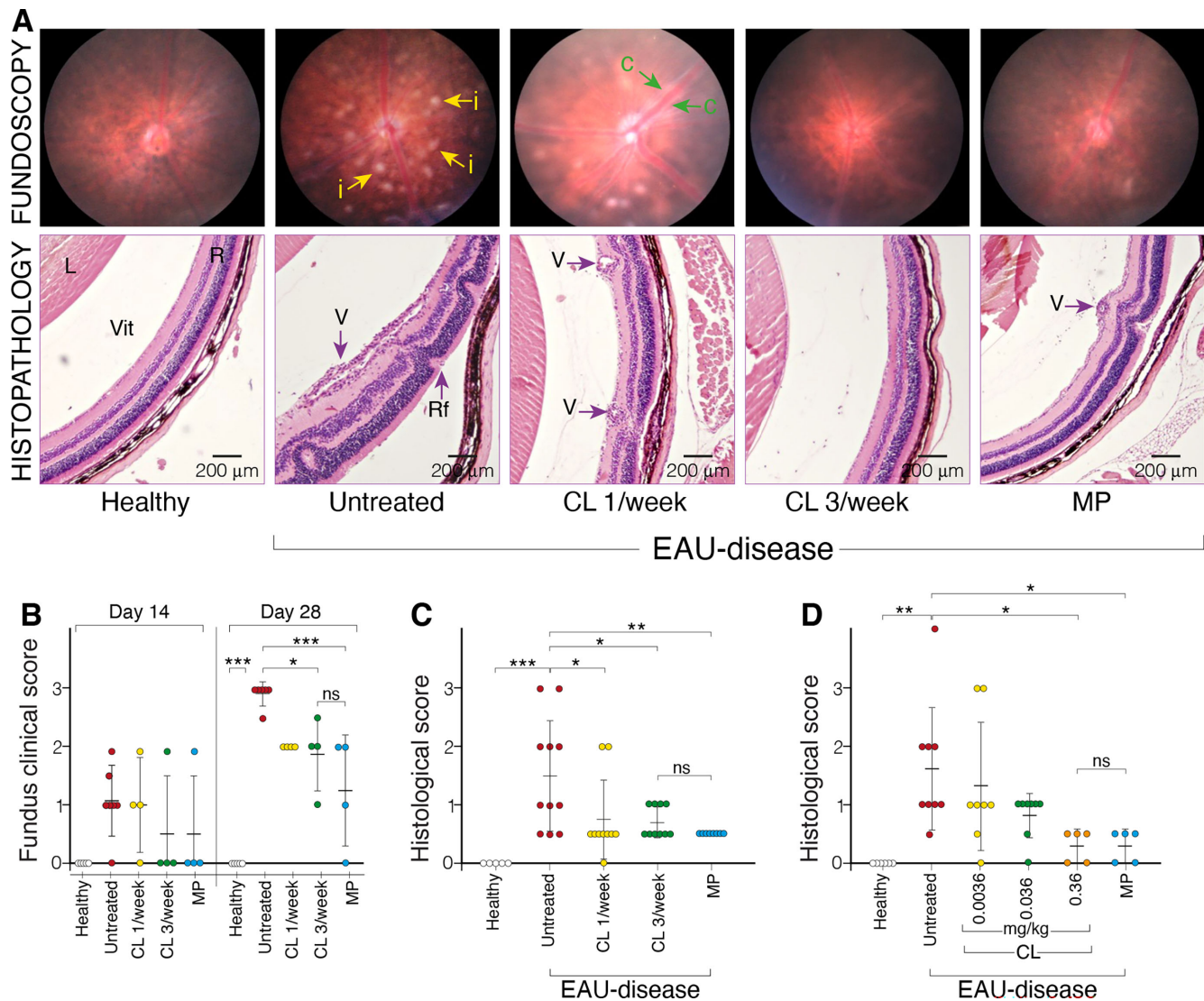


FIGURE 1. Clarstatin ameliorated ocular inflammation in the EAU C57BL/6J mice model; it was evaluated at two dosing regimens using clinical and histological scoring. The tested groups consisted of healthy, wild-type mice; EAU-disease untreated mice (control); mice treated by Clarstatin IP injection (CL; 0.18 mg/kg) once a week or three times a week; or mice treated with methylprednisolone IP injection (MP; 20 mg/kg) three times a week. (A, top) Fundus images photographed by the MICRON III 4 weeks after induction of EAU indicating attenuation of retinal inflammation by Clarstatin, characterized by fewer foci of retinal infiltrates, indicated by yellow arrows (i). The green arrows (c) point to perivascular cuffing indicative of retinal vasculitis. (A, bottom) Representative H&E staining sections of the retina of the right eyes of the mice, 35 days after induction of EAU. L, lens; Vit, vitreous; R, retina; Rf, retinal fold; V, vasculitis. Scale bars: 200 μ m. (B) Quantitation of the fundus clinical scores 14 and 28 days after EAU induction. (C) Quantitation of the histopathological scores in individual mouse eye sections 35 days after EAU induction. (D) Dose-dependent therapeutic effect of Clarstatin administrated once a week at three different doses (0.0036, 0.036, and 0.36 mg/kg) and evaluated by histopathology score 35 days after EAU induction. The graph indicates that Clarstatin considerably reduced the structural damage. Each data point represents an eye, and the mean score per treatment group is indicated with error bars computed as SEMs from three independent experiments. Comparisons were performed by one-way ANOVA with Tukey's multiple-comparisons test. * $P < 0.05$, ** $P \leq 0.01$, *** $P \leq 0.001$; ns, not significant ($P \geq 0.05$).

EAU-disease mouse, and a Clarstatin-treated mouse (0.036 mg/kg) 35 days after immunization. The immunoreactivity of the CD45⁺ pan-leukocyte biomarker (red fluorescence) and calreticulin (green fluorescence) was assessed (Fig. 2A). Scarce positive CD45 immunoreactivity was noted in the wild-type (healthy) and Clarstatin-treated mice. By contrast, marked CD45 immunoreactivity was observed in the EAU-disease mouse in the ganglion cell layer (GCL), inner nuclear layer (INL), outer nuclear layer (ONL), and photoreceptor inner segment (PIS) layer. Calreticulin immunoreactivity was

noted in the wild-type and Clarstatin-treated mice in the GCL, PIS layer, retinal pigment epithelium, and choroidal outer layer. In EAU-disease mouse, its expression was significantly increased in the GCL. Its immunoreactivity also appeared in the INL and ONL. Distortion of photoreceptor inner and outer segment layers was noted in EAU-disease mouse. The marked reduction in CD45 immunoreactivity in Clarstatin-treated mouse indicates reduced infiltration and accumulation of CD45⁺ leukocytes with preservation of photoreceptor segments. Colocalization between

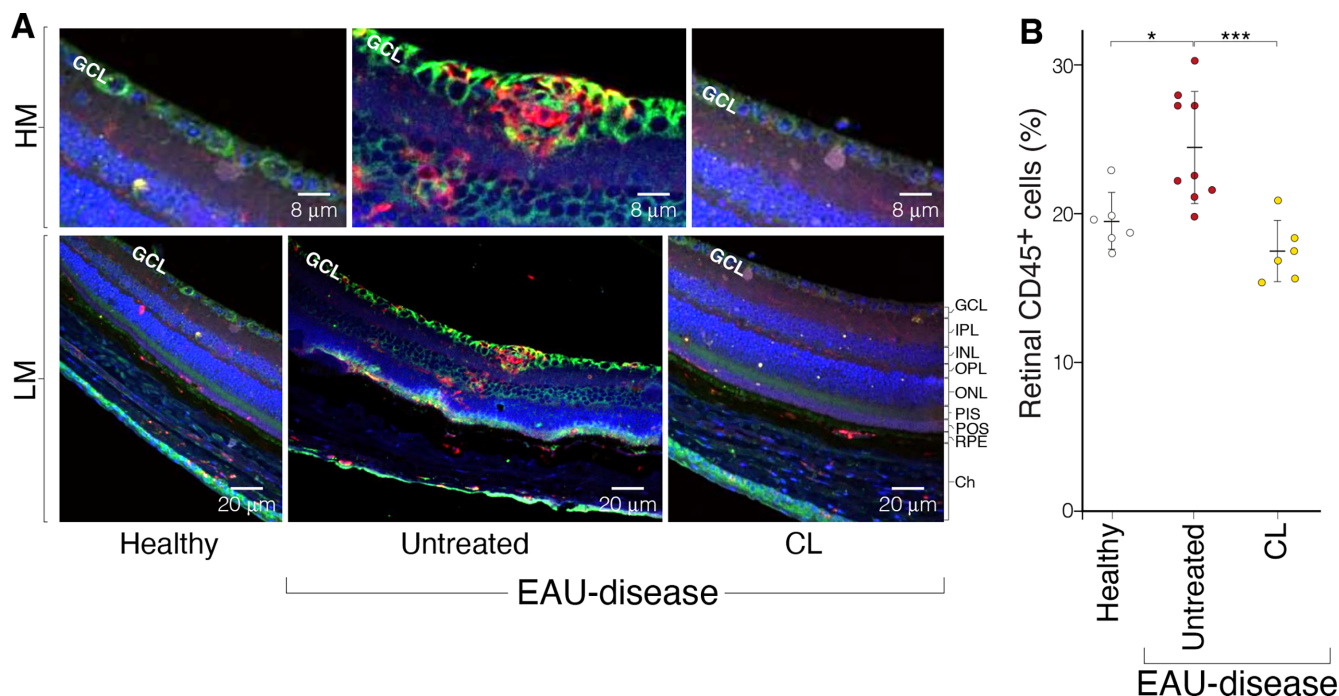


FIGURE 2. Clarstatin inhibited retinal infiltration of leukocytes in EAU-disease C57BL/6J mice, evaluated by immunostaining and flow cytometry. The tested groups consisted of untreated wild-type mice (healthy), EAU-disease untreated mice (control), or Clarstatin-treated mice (CL; 0.036 mg/kg, IP twice a week). **(A)** Representative microscopical immunostaining images of individual mouse retinal paraffin sections 35 days after EAU induction at low magnification (LM, bottom) and at high magnification (HM, top) stained red for leukocytes expressing CD45 pan-leukocyte biomarker and green for calreticulin. Scale bars: 20 μ m (bottom) and 8 μ m (top). Scarce positive CD45 staining is noted in the healthy and Clarstatin-treated mice. CD45 staining was noted in the EAU-disease mouse in the GCL, INL, ONL, and PIS layer. Calreticulin staining was noted in the wild-type and Clarstatin-treated mice in the GCL, PIS layer, retinal pigment epithelium (RPE), and choroidal outer layer. In EAU-disease mice, its expression was significantly increased in the GCL and appeared in the INL and ONL. Distortion of photoreceptor inner and outer segment layers was noted in EAU-disease mice. Co-localization between calreticulin-expressing cells and CD45⁺ cells was noted in the GCL and INL. **(B)** Quantitation of the therapeutic effect of Clarstatin based on FACS analysis for the percentage of CD45⁺ expressing cells in the retina. Results are shown as scattergraphs of the percentage of cells per sample indicated by all symbols. The means of all samples are indicated by the bars, and error bars indicate SEMs from three independent experiments. Comparisons were performed by one-way ANOVA with Tukey's multiple-comparisons test. * $P < 0.05$, *** $P < 0.001$.

calreticulin-expressing cells and CD45⁺ cells was noted in the GCL and INL. FACS analyses further indicated that treatment with Clarstatin (0.036 mg/kg), for 5 weeks, significantly reduced by 28% ($P < 0.001$) retinal levels of CD45⁺ cells, compared to untreated EAU-disease mice, indicative of an inhibitory effect on leukocyte infiltration into the retina (Fig. 2B).

To gain insight into whether there was an effect of Clarstatin on the peripheral expression levels of CD45⁺/CD4⁺ T cells in the spleen of EAU-disease C57BL/6J mice, FACS was performed on splenocytes derived from the wild-type mice, EAU-disease mice, Clarstatin-treated mice (0.18 mg/kg Clarstatin once or three times a week, IP) or methylprednisolone-treated mice (20 mg/kg) (Fig. 3). Clarstatin significantly reduced by 38% ($P < 0.05$) and 51% ($P < 0.001$) the expression levels of CD4⁺ cells in the spleen of mice treated with Clarstatin once and three times a week, respectively, compared to EAU-disease untreated mice, similar to corticosteroid-treated mice in which there was a 47% reduction ($P < 0.01$) in CD4⁺ cell levels expression. These results further support the proposal that the reduced ocular inflammation and pathology in EAU C57BL/6J mice by Clarstatin was temporally related to its inhibitory effect on retinal infiltration of CD45⁺ leukocytes and decreased peripheral spleen expression of CD4⁺ T cells.

Systemic Treatment With Clarstatin, Like Corticosteroids, Decreased Ocular Cytokine Levels

The cytokine IL-6 is consistently found in the vitreous of patients with active uveitis and in EAU rodent models,^{31,32} together with other proinflammatory chemokines, such as MCP-1.^{33,34} Specific ELISAs were used to measure their ocular expression levels to investigate the effects of Clarstatin on these proinflammatory biomarkers (Fig. 4). IL-6 and MCP-1 ocular levels were increased by two- and ninefold in EAU-disease eyes, respectively, compared to wild-type mice. Clarstatin and methylprednisolone treatment significantly decreased by 41% ($P < 0.01$) and 38% ($P < 0.01$), respectively, the expression levels of IL-6 and by 59% ($P < 0.05$) and 60% ($P < 0.05$), respectively, the expression level of MCP-1 compared to EAU-disease, untreated mice. These results provide additional evidence of the anti-inflammatory effects of Clarstatin in the EAU C57BL/6J mice model.

Clarstatin Ameliorated Ocular Pathology and Reduced Retinal Infiltration of CD45⁺ Leukocytes in the EAU B10RIII Severe Mice Model

B10RIII female mice were immunized with IRBP(161–180) and PTX to induce acute, severe EAU disease.³⁵ The tested

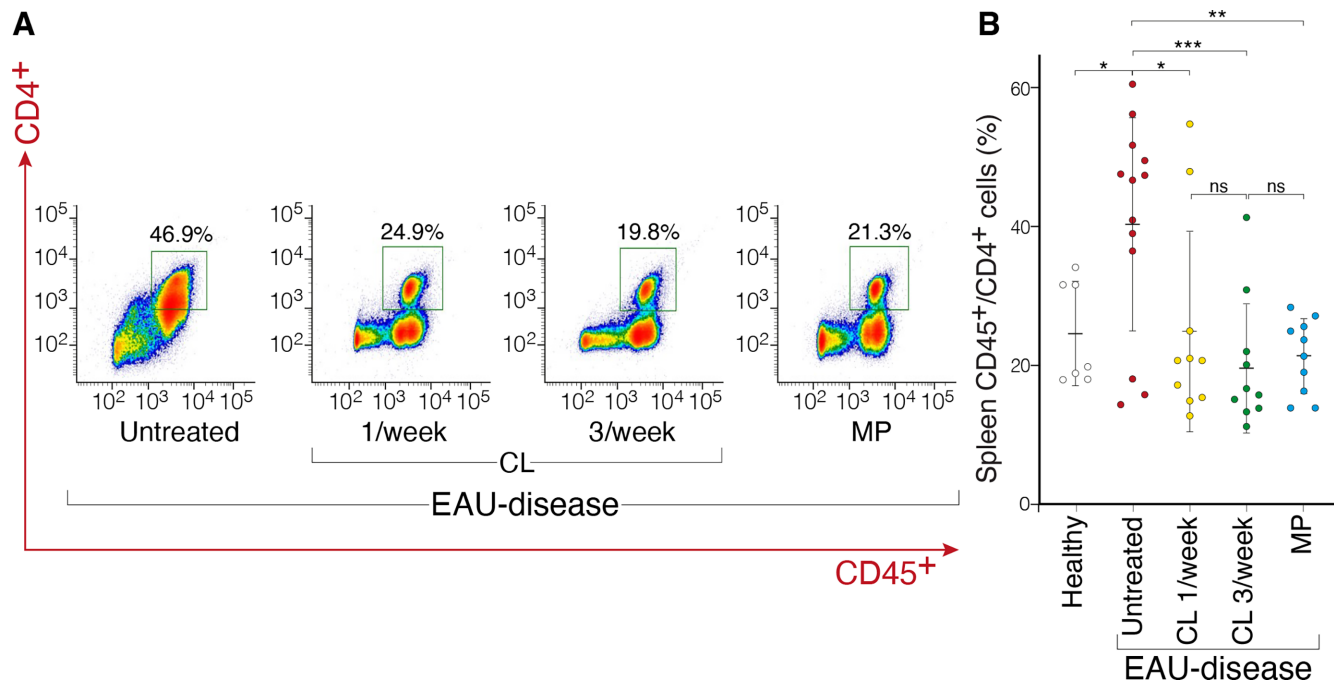


FIGURE 3. Clarstatin inhibited the expression levels of CD45⁺/CD4⁺ T cells in the spleen of EAU-disease C57BL/6J mice, as evaluated by flow cytometry. The tested groups consisted of untreated wild-type mice (healthy), EAU-disease untreated mice (control), or Clarstatin-treated mice (CL; 0.18 mg/kg IP once or three times a week), and methylprednisolone-treated mice (MP, 20 mg/kg, IP three times a week). **(A)** Spleen cells from one mouse per treatment group were measured by flow cytometry on the gate of CD45⁺/CD4⁺ T cells, demonstrating increased expression in EAU-disease untreated mice and significant decreases in CL and MP-treated mice. **(B)** Quantitative results of the percentages of CD45⁺/CD4⁺ T-cell populations per sample indicated by all symbols. The means of all samples are indicated by the bars, and error bars indicate the SEMs. Comparisons were performed by one-way ANOVA with Tukey's multiple-comparisons test. * $P < 0.05$, ** $P < 0.01$, *** $P < 0.001$; ns, not significant ($P \geq 0.05$).

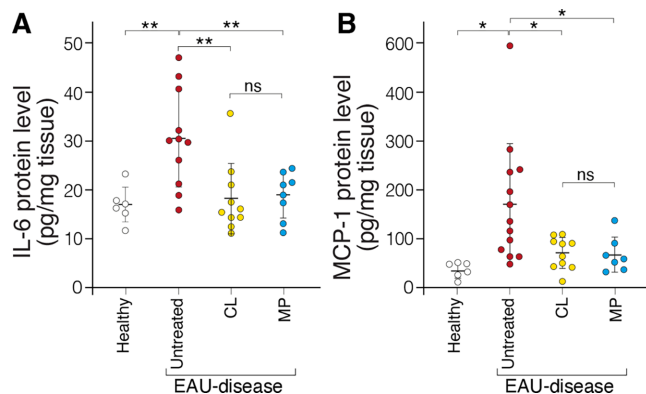


FIGURE 4. **(A, B)** Clarstatin decreased the ocular cytokine concentrations in EAU-disease C57BL/6J mice as evaluated by ELISA. The IL-6 **(A)** and MCP-1 **(B)** expression levels (pg/mg weight eye tissue) were measured by ELISA. The tested groups consisted of untreated naïve mice (healthy), EAU-disease untreated mice (control), Clarstatin-treated mice (CL, 0.18 mg/kg, IP three times a week), and methylprednisolone-treated mice (MP, 20 mg/kg, IP three times a week). Each point represents one mouse. The means of all samples are indicated by the bars, and error bars indicate the SEMs. Samples were run in duplicate, and the mean concentrations were analyzed. IL-6 and MCP-1 were significantly higher in the EAU-disease untreated mice compared to wild-type mice and were significantly reduced upon CL and MP treatment. Comparisons were performed by one-way ANOVA with Tukey's multiple-comparisons test. * $P < 0.05$, ** $P < 0.01$; ns, not significant ($P \geq 0.05$).

groups consisted of wild-type mice (healthy), EAU-disease untreated mice, Clarstatin-treated mice (by IP injection with 0.36 and 1 mg/kg, three times a week for 2 weeks), or methylprednisolone-treated mice (20 mg/kg, three times a week for 2 weeks). Quantitation of the therapeutic effects of Clarstatin was based on EAU scores from the histopathological sections (Fig. 5A). EAU mice developed the disease with an average score of 3.7 ($P < 0.001$), but wild-type mice presented a score of 0. The histopathological analysis indicated improvement in Clarstatin-treated mice (2.4; $P < 0.05$) and corticosteroid-treated mice (1.9; $P < 0.01$), with a significant decrease in the histopathological scores by 36%, and 48%, respectively, when compared to EAU-disease, untreated mice.

To evaluate the impact of Clarstatin on the inflammatory CD45⁺ cell infiltrate, retinas were collected on day 14 for immunological characterization by FACS (Figs. 5B, 5C). Clarstatin at doses of 0.36 mg/kg and 1 mg/kg significantly reduced the CD45⁺ cell levels in the retinas of treated mice compared to untreated mice by 48% ($P < 0.05$). There was no significant difference between the two Clarstatin treatment groups regarding the percentage of CD45⁺ cell levels in the retina, and the Clarstatin effect was comparable to that of the corticosteroids that significantly reduced CD45⁺ retinal cell levels by 58% ($P < 0.05$). Cumulatively, these results indicate that Clarstatin significantly inhibited the leukocyte retinal CD45⁺ cell infiltration and resultant structural damage in the severe EAU model of B10RIII mice.

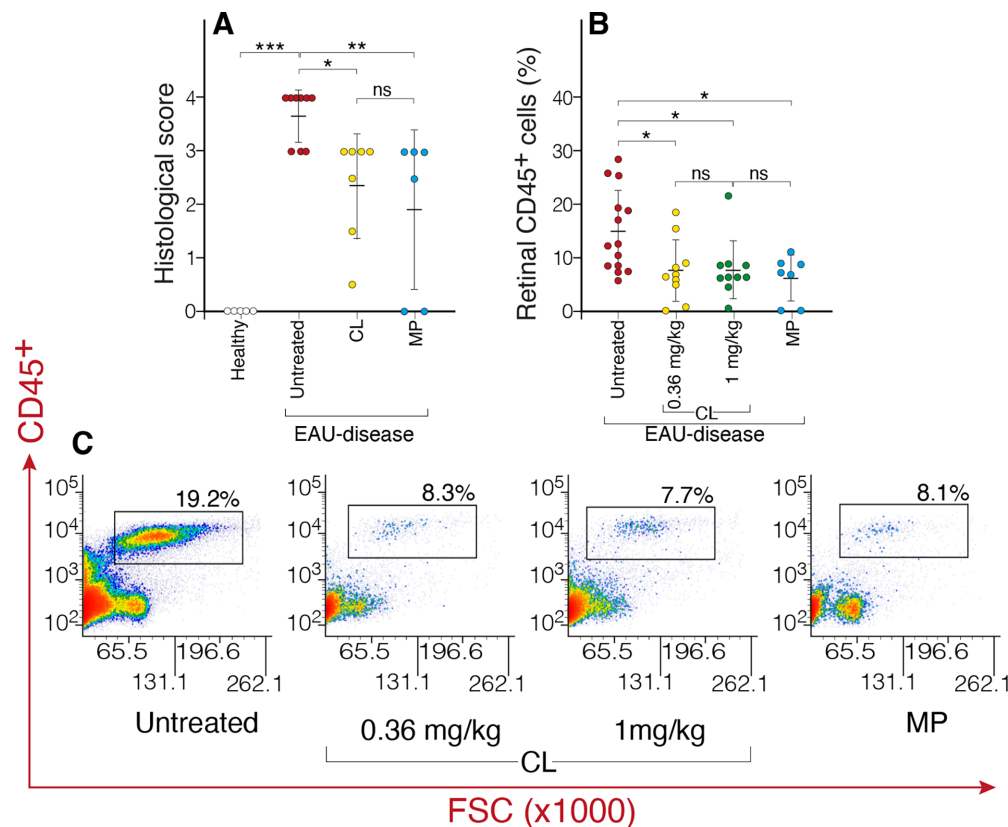


FIGURE 5. Clarstatin ameliorated ocular pathology and reduced retinal infiltration of CD45⁺ leukocytes in the EAU B10RIII severe mice model, as evaluated by histological scoring and flow cytometry. The tested groups consisted of untreated naïve mice (healthy), EAU-disease untreated mice (control), Clarstatin-treated mice (CL; 0.36 mg/kg and 1 mg/kg, IP three times a week), and methylprednisolone-treated mice (MP, 20 mg/kg, IP three times a week). **(A)** Quantitation of the histopathological scores in individual mouse eye sections 14 days after EAU induction indicates the therapeutic effects of CL and MP. Each data point represents an eye, and the mean score per treatment group is indicated with *error bars* computed as SEMs from three independent experiments. Comparisons were performed by one-way ANOVA with Tukey's multiple-comparisons test. * $P < 0.05$, ** $P \leq 0.01$, *** $P \leq 0.001$; ns, not significant ($P \geq 0.05$). **(B)** Quantitation of the therapeutic effect of Clarstatin based on FACS analysis for the percentage of CD45⁺-expressing cells on the retina. Results are shown as scattergraphs of the percentage of cells per sample indicated by all symbols. The means of all samples are indicated by the *bars*, and *error bars* indicate SEMs from three independent experiments. Comparisons were performed by one-way ANOVA with Tukey's multiple-comparisons test. * $P < 0.05$, ** $P < 0.01$, *** $P < 0.001$; ns, not significant ($P \geq 0.05$). **(C)** Retinal CD45⁺ cells from one mouse per treatment group were measured by flow cytometry on the gate of CD45⁺, demonstrating increased expression in the EAU-disease untreated group and significant decreases in the CL and MP-treated mice groups.

DISCUSSION

In the present study, we characterized the therapeutic efficacy of Clarstatin in controlling ocular inflammation in EAU which is a well-established mice model of posterior uveitis that recapitulates key features associated with severe vision loss in humans, including vitritis, retinal vasculitis, and chorioretinitis.³⁶ Central to disease pathogenesis in EAU is retinal infiltration of leukocytes from the periphery and increased ocular expression of typical proinflammatory cytokines inducing distinct histopathological changes.³⁷ In the present study, Clarstatin, in a dose range between 0.18 mg/kg and 1 mg/kg, delivered IP once or three times a week, ameliorated ocular inflammation and inhibited retinal infiltration of CD45⁺ leukocytes in EAU C57BL/6J mild and EAU B10RIII severe mice models. This finding indicates a reduction of the different leukocyte subtypes infiltrating the retina, as CD45⁺ is a leukocyte common antigen. Moreover, Clarstatin decreased peripheral spleen expression of CD4⁺ T cells and ocular expression levels of the proinflammatory cytokine IL-6 and chemokine MCP-1 in the EAU

C57BL/6J mice. These findings indicate that Clarstatin exerts both local effects on the eye and systemic effects in the spleen. Clarstatin effects were similar to those of methylprednisolone, the first-line therapy in noninfectious posterior uveitis,³⁸ and included anti-inflammatory, immunosuppressive effects in EAU-disease mice.³⁹

The major histocompatibility complex (MHC) in mice (H2) and humans (HLA) is similar but has several differences, including chromosomal location, length, and tissue distribution. The SE is a set of MHC class II alleles that are genetically linked to rheumatoid arthritis in human and mice.²² The SE is made up of amino acids 70 to 74 of the HLA-DR β chain, which must have the 70Q/D-K/R-x-x-A74 sequence to be considered part of the SE family.²² The SE is located near the apex of α helical tridimensional structural motif that has been preserved throughout the entire MHC gene family in vertebrates and acts as a signal transduction ligand that binds CS-CRT, triggering NO-mediated prooxidative signaling.⁴⁰ The SE binding site on CRT has previously been mapped to amino acid residues 217 to 223 in the P-domain of CRT. Upon interaction with CRT in dendritic

cells, the SE activates immune regulatory events, among them increased secretion of IL-6.⁴¹ The SE is expressed in all haplotypes and therefore we hypothesize that Clarstatin will target all H2 mice haplotype alpha chains blocking the interaction with CS-CRT.

CRT is expressed at the cell surface of activated human peripheral blood T lymphocytes, where it is physically associated with a pool of unfolded HLA molecules. It was shown that both CD8⁺ and CD4⁺ T lymphocytes expressed CRT in the plasma membrane.⁴² Pathophysiological roles of CRT in autoimmune disease contribute to the associated inflammation.¹⁹ CRT, with its widespread tissue distribution, is also present as a unique isoform in the retina⁴³: neurons, Müller glia, retinal epithelial cells associated with melanin-containing pigment granules, and retinal endothelial cells.⁴⁴ CRT cell surface exposure during inflammation is required for phagocytosis of neurons by activated microglia.⁴⁵ Indeed, the immunostaining sections of the retina (Fig. 2A) in EAU-disease mice indicated high expression of CRT in the GCL and INL. The tight co-localization of infiltrating CD45⁺ leukocytes to CRT-expressing cells may suggest that CS-CRT may activate the innate immune response being expressed as an early marker of apoptosis.⁴⁶ Therefore, we hypothesize that Clarstatin, by inhibiting HLA-DRB SE-CRT activation, may cause attenuation of leukocyte inflammatory properties. Clarstatin may confer these anti-inflammatory cellular effects by targeting the main pathological molecular mechanisms of HLA-activated CRT: (1) CRT-dependent modulation of Ca²⁺ signaling may contribute to inhibition of the T-cell-mediated adaptive immune response.⁴⁷ (2) Modulation of CRT binding to the specific promoter–glucocorticoid response element⁴⁸ may inhibit CRT-induced changes in gene expression, leading to a corticosteroid-like immunosuppressive effect. (3) Blocking the intracellular COOH-terminal region of the activated integrin α subunits that contain a highly conserved amino acid sequence, to which CRT as a potential integrin regulator binds, resulting in decreased leukocyte cell adhesion and/or migration.⁴⁹ Regulatory T cells (Tregs) are essential for maintaining immune balance and preventing autoimmune diseases. Although our study did not directly examine Treg levels in treated versus untreated mice, we speculate that changes in Treg levels may have occurred secondary to changes in the level of ocular cytokines—namely, IL-6. IL-6 is one of the main inflammatory cytokines, with pleiotropic functions and effects on various immunocytes.⁵⁰ IL-6 was reported to inhibit iTreg differentiation.^{51,52} Studies have demonstrated that IL-6 has a very important role in regulating the balance between IL-17–producing Th17 cells and Tregs. IL-6 induced the development of Th17 cells from naïve T cells together with TGF- β ; in contrast, IL-6 inhibited TGF- β –induced Treg differentiation.⁵³ Increased IL-6 production in graft-versus-host disease (GVHD) has been shown to impair the reconstitution of Tregs. Blocking IL-6 signaling through antibody-mediated inhibition of the IL-6 receptor (IL-6R) significantly reduced GVHD-related damage and led to a marked increase in Treg numbers, driven by both thymic-dependent and thymic-independent mechanisms.⁵⁴ Similarly, we assume that the ability of Clarstatin to lower intraocular IL-6 may have supported Treg reconstitution, thereby reducing disease severity. In the present study, Clarstatin ameliorated the retinal pathology subsequent to inhibition of CD45⁺/CD4⁺ inflammatory cell recruitment and infiltration into the eye. Therefore, it is reasonable to propose that Clarstatin inhibits the process of inflammatory cell recruitment to the eye via multiple pharmacodynamic

mechanisms of action as mentioned above. Because of the involvement of CRT in uveitis and other systemic inflammatory disorders, its blockade represents a potential new modality of therapy.

Limitations of the current study include a lack of data on different modes of delivery of Clarstatin and its biodistribution in mice tissues, as well as data on HLA–CRT interaction in the EAU model, which are a gap in our full understanding of the molecular mechanisms involved in the anti-inflammatory effect of Clarstatin. Based on the results of the study, it is reasonable to propose that the therapeutic effects of Clarstatin include inhibition of the innate and adaptive immune response. Further studies are required in order to better delineate and understand the specific immunological pathway through which Clarstatin exerts its effects, including the effect of Clarstatin on antigen-specific T cells. Future investigations should aim to directly assess Treg levels and functionality in response to Clarstatin treatment to further elucidate its immunomodulatory mechanisms in EAU. In our study, we focused on the effects of Clarstatin during the induction phase of EAU. However, we did not evaluate the therapeutic effect of Clarstatin during the effector phase of EAU, which is a limitation of our research. We recognize the importance of assessing its impact in this phase and plan to address it in future studies. Additionally, we did not investigate systemic cytokine profiles, including IFN- γ and IL-17, in the spleen or draining lymph nodes. This is another limitation of our study, as understanding these cytokine responses is crucial to elucidating the mechanism of action of Clarstatin in EAU. We intend to explore these aspects in subsequent investigations.

In summary, this study provides preclinical evidence that systemic treatment with Clarstatin significantly suppresses EAU in mice, similar to corticosteroid treatment. These results propose that Clarstatin potentially represents an effective alternative or adjunct therapy to corticosteroids for treatment of autoimmune uveitis in humans.

Acknowledgments

The authors thank Zehava Cohen for help with the artwork.

Supported by the Hebrew University of Jerusalem-Yissum Intramural Research Funds and by a Kamin grant (67970) from the Israel Innovation Authority.

Disclosure: **S. Merzbach**, None; **A. Schumacher-Klinger**, None; **M. Klazas**, None; **A. Hoffman**, None; **P. Lazarovici**, None; **C. Gilon**, None; **G. Nussbaum**, None; **R. Amer**, None

References

1. Prete M, Dammacco R, Fatone MC, Racanelli V. Autoimmune uveitis: clinical, pathogenetic, and therapeutic features. *Clin Exp Med*. 2016;16(2):125–136.
2. Gritz DC, Wong IG. Incidence and prevalence of uveitis in Northern California; the Northern California epidemiology of uveitis study. *Ophthalmology*. 2004;111(3):491–500.
3. Ghadiri N, Reekie IR, Gordon I, et al. Systematic review of clinical practice guidelines for uveitis. *BMJ Open Ophthalmol*. 2023;8(1):e001091.
4. Mehta NS, Emami-Naeini P. A review of systemic biologics and local immunosuppressive medications in uveitis. *J Ophthalmic Vis Res*. 2022;17(2):276–289.

5. Thng ZX, Bromeo AJ, Mohammadi SS, et al. Recent advances in uveitis therapy: focus on selected phase 2 and 3 clinical trials. *Expert Opin Emerg Drugs*. 2023;28(4):297–309.
6. Klaska I, Forrester J. Mouse models of autoimmune uveitis. *Curr Pharm Des*. 2015;21(18):2453–2467.
7. Agarwal RK, Silver PB, Caspi RR. Rodent models of experimental autoimmune uveitis. *Methods Mol Biol*. 2012;900:443–469.
8. Forrester J. Uveitis: pathogenesis. *Lancet*. 1991;338(8781):1498–1501.
9. Kerr EC, Copland DA, Dick AD, Nicholson LB. The dynamics of leukocyte infiltration in experimental autoimmune uveoretinitis. *Prog Retin Eye Res*. 2008;27(5):527–535.
10. Merzbach S, Hoffman A, Lazarovici P, Gilon C, Amer R. Development of Clarstatin, a novel drug lead for the therapy of autoimmune uveitis. *Pharmaceutics*. 2024;16(6):723.
11. Gregersen PK, Silver J, Winchester RJ. The shared epitope hypothesis. An approach to understanding the molecular genetics of susceptibility to rheumatoid arthritis. *Arthritis Rheum*. 1987;30(11):1205–1213.
12. Caspi RR, Dick A, Forrester J, et al. Immunology of uveitis. In: Zierhut M, Pavesio C, Ohno S, Orefice F, Rao N, eds. *Intraocular Inflammation*. Berlin: Springer; 2016:39–81.
13. Hou S, Li N, Liao X, Kijlstra A, Yang P. Uveitis genetics. *Exp Eye Res*. 2020;190:107853.
14. Shindo Y, Inoko H, Yamamoto T, Ohno S. HLA-DRB1 typing of Vogt-Koyanagi-Harada's disease by PCR-RFLP and the strong association with DRB1*0405 and DRB1*0410. *Br J Ophthalmol*. 1994;78(3):223–226.
15. Levinson RD, Park MS, Rikkers SM, et al. Strong associations between specific HLA-DQ and HLA-DR alleles and the tubulointerstitial nephritis and uveitis syndrome. *Invest Ophthalmol Vis Sci*. 2003;44(2):653–657.
16. Ling S, Cheng A, Pumpens P, Michalak M, Holoshitz J. Identification of the rheumatoid arthritis shared epitope binding site on calreticulin. *PLoS One*. 2010;5(7):e11703.
17. Ling S, Pi X, Holoshitz J. The rheumatoid arthritis shared epitope triggers innate immune signaling via cell surface calreticulin. *J Immunol*. 2007;179(9):6359–6367.
18. Eggleton P, Bremer E, Dudek E, Michalak M. Calreticulin, a therapeutic target? *Expert Opin Ther Targets*. 2016;20(9):1137–1147.
19. Eggleton P, Llewellyn DH. Pathophysiological roles of calreticulin in autoimmune disease. *Scand J Immunol*. 1999;49(5):466–473.
20. Naveh S, Tal-Gan Y, Ling S, Hoffman A, Holoshitz J, Gilon C. Developing potent backbone cyclic peptides bearing the shared epitope sequence as rheumatoid arthritis drug-leads. *Bioorg Med Chem Lett*. 2012;22(1):493–496.
21. Fu J, Ling S, Liu Y, et al. A small shared epitope-mimetic compound potentially accelerates osteoclast-mediated bone damage in autoimmune arthritis. *J Immunol*. 2013;191(5):2096–2103.
22. Ling S, Liu Y, Fu J, Colletta A, Gilon C, Holoshitz J. Shared epitope-antagonistic ligands: a new therapeutic strategy in mice with erosive arthritis. *Arthritis Rheumatol*. 2015;67(8):2061–2070.
23. Avichezer D, Silver PB, Chan CC, Wiggert B, Caspi RR. Identification of a new epitope of human IRBP that induces autoimmune uveoretinitis in mice of the H-2b haplotype. *Invest Ophthalmol Vis Sci*. 2000;41(1):127–131.
24. Okada AA, Sakai JI, Usui M, Mizuguchi J. Intraocular cytokine quantification of experimental autoimmune uveoretinitis in rats. *Ocul Immunol Inflamm*. 1998;6(2):111–120.
25. Thureau SR, Chan CC, Nussenblatt RB, Caspi RR. Oral tolerance in a murine model of relapsing experimental autoimmune uveoretinitis (EAU): induction of protective tolerance in primed animals. *Clin Exp Immunol*. 1997;109(2):370–376.
26. Eltoum I, Fredenburgh J, Myers RB, Grizzle WE. Introduction to the theory and practice of fixation of tissues. *J Histotechnol*. 2001;24(3):173–190.
27. Fu Q, Man X, Wang X, et al. CD83⁺ CCR7⁺ NK cells induced by interleukin 18 by dendritic cells promote experimental autoimmune uveitis. *J Cell Mol Med*. 2019;23(3):1827–1839.
28. Makhoul M, Dewispelaere R, Relvas LJ, et al. Characterization of retinal expression of vascular cell adhesion molecule (VCAM-1) during experimental autoimmune uveitis. *Exp Eye Res*. 2012;101:27–35.
29. Epps SJ, Boldison J, Stimpson ML, et al. Re-programming immunosurveillance in persistent non-infectious ocular inflammation. *Prog Retin Eye Res*. 2018;65:93–106.
30. Chen YH, Lightman S, Calder VL. CD4⁺ T-cell plasticity in non-infectious retinal inflammatory disease. *Int J Mol Sci*. 2021;22(17):9584.
31. Perez VL, Papaliodis GN, Chu D, Anzaar F, Christen W, Foster CS. Elevated levels of interleukin 6 in the vitreous fluid of patients with pars planitis and posterior uveitis: the Massachusetts Eye & Ear experience and review of previous studies. *Ocul Immunol Inflamm*. 2004;12(3):205–214.
32. Tode J, Richert E, Koinzer S, et al. Intravitreal injection of anti-interleukin (IL)-6 antibody attenuates experimental autoimmune uveitis in mice. *Cytokine*. 2017;96:8–15.
33. Verma MJ, Lloyd A, Rager H, et al. Chemokines in acute anterior uveitis. *Curr Eye Res*. 1997;16(12):1202–1208.
34. Crane IJ, McKillop-Smith S, Wallace CA, Lamont GR, Forrester JV. Expression of the chemokines MIP-1 α , MCP-1, and RANTES in experimental autoimmune uveitis. *Invest Ophthalmol Vis Sci*. 2001;42(7):1547–1552.
35. Silver PB, Rizzo IV, Chan CC, Donoso LA, Wiggert B, Caspi RR. Identification of a major pathogenic epitope in the human IRBP molecule recognized by mice of the H-2r haplotype. *Invest Ophthalmol Vis Sci*. 1995;36(5):946–954.
36. Yang JM, Yun KA, Jeon J, et al. Multimodal evaluation of an interphotoreceptor retinoid-binding protein-induced mouse model of experimental autoimmune uveitis. *Exp Mol Med*. 2022;54(3):252–262.
37. Ferreira LB, Williams KA, Best G, Haydinger CD, Smith JR. Inflammatory cytokines as mediators of retinal endothelial barrier dysfunction in non-infectious uveitis. *Clin Transl Immunol*. 2023;12(12):e1479.
38. Valdes LM, Sobrin L. Uveitis therapy: the corticosteroid options. *Drugs*. 2020;80(8):765–773.
39. Li H, Gao Y, Xie L, et al. Prednisone reprograms the transcriptional immune cell landscape in CNS autoimmune disease. *Front Immunol*. 2021;12:739605.
40. De Almeida DE, Ling S, Holoshitz J. New insights into the functional role of the rheumatoid arthritis shared epitope. *FEBS Lett*. 2011;585(23):3619–3626.
41. Holoshitz J, De Almeida DE, Ling S. A role for calreticulin in the pathogenesis of rheumatoid arthritis. *Ann N Y Acad Sci*. 2010;1209(1):91–98.
42. Arosa FA, De O, Porto G, Carmo AM, De Sousa M. Calreticulin is expressed on the cell surface of activated human peripheral blood T lymphocytes in association with major histocompatibility complex class I molecules. *J Biol Chem*. 1999;274(24):16917–16922.
43. Opas M, Michalak M. Calcium storage in nonmuscle tissues: is the retina special? *Biochem Cell Biol*. 1992;70(10–11):972–979.
44. Zamora DO, Riviere M, Choi D, et al. Proteomic profiling of human retinal and choroidal endothelial cells reveals molecular heterogeneity related to tissue of origin. *Mol Vis*. 2007;13:2058–2065.
45. Fricker M, Oliva-Martín MJ, Brown GC. Primary phagocytosis of viable neurons by microglia activated with LPS or

- $A\beta$ is dependent on calreticulin/LRP phagocytic signalling. *J Neuroinflammation*. 2012;9:1–12.
46. Grimsley C, Ravichandran KS. Cues for apoptotic cell engulfment: eat-me, don't-eat-me and come-get-me signals. *Trends Cell Biol*. 2003;13(12):648–656.
 47. Porcellini S, Traggiai E, Schenk U, et al. Regulation of peripheral T cell activation by calreticulin. *J Exp Med*. 2006;203(2):461–471.
 48. Burns K, Duggan B, Atkinson EA, et al. Modulation of gene expression by calreticulin binding to the glucocorticoid receptor. *Nature*. 1994;367(6462):476–480.
 49. Ohkuro M, Kim JD, Kuboi Y, et al. Calreticulin and integrin α dissociation induces anti-inflammatory programming in animal models of inflammatory bowel disease. *Nat Commun*. 2018;9(1):1982.
 50. Hunter CA, Jones SA. IL-6 as a keystone cytokine in health and disease. *Nat Immunol*. 2015;16(5):448–457.
 51. Bettelli E, Carrier Y, Gao W, et al. Reciprocal developmental pathways for the generation of pathogenic effector TH17 and regulatory T cells. *Nature*. 2006;441(7090):235–238.
 52. Zhou L, Lopes JE, Chong MMW, et al. TGF- β -induced Foxp3 inhibits T(H)17 cell differentiation by antagonizing ROR γ t function. *Nature*. 2008;453(7192):236–240.
 53. Kimura A, Kishimoto T. IL-6: regulator of Treg/Th17 balance. *Eur J Immunol*. 2010;40(7):1830–1835.
 54. Chen X, Das R, Komorowski R, et al. Blockade of interleukin-6 signaling augments regulatory T-cell reconstitution and attenuates the severity of graft-versus-host disease. *Blood*. 2009;114(4):891–900.